

# Short-Duration Autoignition Temperature Measurements For Hydrocarbon Fuels Near Heated Metal Surfaces

KERMIT C. SMYTH and NELSON P. BRYNER

*National Institute of Standards and Technology, Building and Fire  
Research Laboratory, Gaithersburg, Maryland 20899*

*(Received 11 October 1996; In final form 13 March 1997)*

An apparatus has been designed, built, and extensively tested for making short-duration autoignition temperature measurements of hydrocarbon fuels under atmospheric pressure conditions where the fuel/air stoichiometry, the nature of the hot metal surface, and the contact time between the fuel/air mixture and the heated surface are well controlled. This approach provides a much more reliable database to establish the importance of fuel structure and surface effects on measured autoignition temperatures than the current ASTM E659 procedure, which involves variable ignition delay times and unspecified stoichiometries for ignition in a heated glass flask. Two series of tests have been conducted: (1) over 1100 individual autoignition temperature determinations for the ignition of 15 hydrocarbon fuels containing 1 to 8 carbon atoms on heated nickel, stainless steel, and titanium surfaces for three different stoichiometries ( $\phi = 0.7, 1.0$  and  $1.3$ ); and (2) ~190 determinations for 10 linear and branched alkanes on heated nickel for stoichiometric conditions. Excellent repeatability has been achieved within a given series of measurements, and good replicate values have been obtained for data collected on separate days.

Autoignition temperatures measured under short-contact time conditions are much higher (by typically 500 K or more) than found in most prior investigations, where exposure times were longer and test conditions less well controlled. The autoignition temperatures generally decrease for the larger hydrocarbons and for richer mixtures, although the  $C_2$  hydrocarbons (ethane, ethylene and acetylene) have particularly low values. The highest autoignition temperatures are observed for nickel surfaces and the lowest for stainless steel, with titanium being an intermediate case. Overall, the different metal surfaces exhibit a moderate influence on the observed autoignition temperatures.

Prior experimental and modeling investigations indicate that the branched alkanes should be more resistant to autoignition than the linear isomers, and thus present a reduced hazard. Data obtained in the present study are consistent with this prediction, although the differences in measured autoignition temperatures are typically less than 100 K for isomers containing the same number of carbon atoms.

**Keywords:** Autoignition; hydrocarbon fuels; metal surfaces; nickel; premixed conditions; stainless steel; titanium

## 1. INTRODUCTION

Self-ignition temperatures for hydrocarbon fuels depend on both the molecular structure of the fuel and on the surface material. However, elucidation of the importance of these effects has been hampered by use of the standard ASTM E659 test procedure [1978], which is based upon the apparatus of Setchkin [1954]. In this method, ignition under ambient pressure conditions often requires long and variable times, from typically a few seconds up to several minutes [Setchkin, 1954; Zabetakis *et al.*, 1954]. The capability of varying the material composition of the hot surface is also limited, since borosilicate glass is the only surface used presently. Although liquids are commonly injected into the hot flask, the ASTM standard states that "no condensed phase, liquid or solid, should be present when ignition occurs". Thus, this test measures ignition temperatures for a complex mixture of fuel decomposition products under conditions where both the time to ignition and the composition of the pyrolysis products will vary depending upon the initial temperature selected. A method for measuring autoignition temperatures under better controlled conditions would provide more meaningful data on fuel structure and surface effects. The appropriate time scale of autoignition temperature measurements depends on the particular practical application, which can range from transient events to long-term storage considerations. Of particular interest in the present study are short-duration measurements, which are relevant for evaluating hazards involving brief exposure times, such as those arising from malfunctions and accidents.

In the apparatus described below, a flowing gas-phase fuel/air stream at atmospheric pressure impinges upon a hot surface whose composition and temperature are well controlled. Under these experimental conditions a large number of parameters can influence the measured autoignition temperature [Laurendeau, 1982], including the following:

- fuel structure
  - surface material
  - surface temperature
  - fuel/air stoichiometry
  - 
  - surface size
  - surface orientation
  - initial fuel/air temperature
  - contact or residence time
  - condition of surface
-

- pressure
- heating rate of surface

In the present study the first four parameters have been varied systematically while keeping the others fixed. Prior investigations of Zabetakis *et al.* [1954], Kumagai and Kimura [1957], Zabetakis [1965], Cutler [1974], and Laurendeau [1982] have shown that the contact time between a fuel/air mixture and the heated surface has a dramatic effect upon the observed autoignition temperature, with values increasing sharply with decreasing times. Since fuel decomposition must precede autoignition, shorter contact times require more vigorous heating to create conditions favorable for ignition. However, the specific chemical pathways and resulting decomposition products are sensitive to the particular time-temperature history prior to ignition. The estimated contact time of the present measurements is significantly shorter than times of 2–600 s reported when using the ASTM apparatus [Zabetakis *et al.*, 1954; Mullins, 1955; Zabetakis, 1965; McCracken, 1970; NFPA 325M, 1984; NFPA, 1995]. Therefore, one anticipates that such short duration measurements will result in much higher autoignition temperatures than these earlier determinations.

Experiments have also been carried out in which the influence of the approach velocity of the fuel/air mixture impinging upon the metal surface and the heating rate of the surface were investigated. The key role of stoichiometry has been examined, since autoignition temperatures can vary strongly with the fuel/air mixture ratio, especially for catalytic surfaces such as platinum [Coward and Guest, 1927; Pfefferle *et al.*, 1989a, 1989b]. To establish accurately the fuel structure effects upon ignition temperatures, three different stoichiometric conditions were investigated. In contrast, the conventional ASTM E659 [1978] procedure does not control the fuel/air stoichiometry, since a specified volume of a liquid fuel is injected into the heated flask and then monitored for times up to ten minutes. Thus, the initial stoichiometry varies for different fuel densities, and the stoichiometry can decrease slowly during the test due to fuel loss by diffusion.

Two series of measurements have been conducted. The first included the development and testing of the apparatus [Smyth and Bryner, 1990]. Important issues are: (1) clarifying the effects of surface materials upon autoignition temperatures of hydrocarbon fuels and (2) comparing ASTM test method results with more controlled measurements of autoignition properties. The primary emphasis was on fuel structure effects, so that a reliable database can be established for testing the proposed mechanisms of autoignition. Over 1100 individual autoignition temperature determinations have been made for the

---

ignition of 15 hydrocarbon fuels on heated nickel, stainless steel, and titanium surfaces for three different fuel/air mixtures (stoichiometry  $\phi = 0.7, 1.0$  and  $1.3$ ). The second series was much more limited and was conducted in 1994 with a duplicate apparatus at the Air Force Engineering and Services Center (Tyndall Air Force Base, FL). Here the focus was to compare the autoignition temperatures for 10 linear and branched alkanes on one surface (nickel) and for stoichiometric conditions. Recently, Hamins and Borthwick [1997] have used the 1990 apparatus to investigate the influence of several suppression agents upon the autoignition temperature for stoichiometric methane/air, ethylene/air, and propane/air mixtures impinging upon a nickel surface.

## 2. DESIGN CONSIDERATIONS

An apparatus for measuring autoignition temperatures for short exposure times must be able to heat the ignition surface uniformly and reproducibly up to  $\sim 1500$  K, introduce a specific fuel/air mixture onto the heated surface, and measure the time-temperature history of the surface during the ignition of the fuel. Design considerations include (1) the size of the ignition surface, (2) the orientation of the surface, (3) the method for heating the surface, (4) the fuel delivery system for liquid and gaseous fuels, and (5) the method for measuring surface temperatures.

### 2.1. Ignition Surface Size

Since multiple ignitions for each surface and fuel/air mixture are required in order to establish the precision of the autoignition temperature determinations, keeping the heated area of the ignition surface small is desirable because this reduces the time, fuel, heating, and material requirements. In addition, a small surface can be heated more uniformly than a larger ignition area. Whereas high fuel flow rates are readily obtainable for light hydrocarbon fuels from high-pressure cylinders, such is not the case for liquid fuels. The capabilities for fuel delivery were limited for the heaviest fuels investigated here (see below), thus favoring the use of small ignition surfaces.

### 2.2. Surface Orientation

The orientation of the ignition surface relative to the direction of the fuel/air flow can influence the flow patterns and contact times near the surface. A  $45^\circ$  angle between the surface and the flowing gas stream has the advantage of

minimizing both the thickness of the boundary layer which develops along the surface and the residence time of the fuel/air mixture in contact with the surface. For a fuel/air flow parallel to the surface (i.e.,  $0^\circ$  orientation) and a velocity of 16 cm/s, the laminar boundary layer thickness is estimated [Holman, 1981] to exceed 0.7 cm for a foil length along the flow of 2.06 cm (see Sections 3.1.1 and 3.2.1 for typical experimental conditions). If the surface and the fuel/air flow were perpendicular ( $90^\circ$  orientation), a stagnation point would develop on the flow centerline. This would allow the fuel/air mixture to remain near the surface for extended periods of time, resulting in additional fuel pyrolysis. Such long and ill-defined residence times would create essentially the same problems that currently exist in the conventional ASTM procedure [1978] in that the residence time is variable and poorly controlled.

### 2.3. Heating the Ignition Surface

Heating a small surface to 1500 K can be accomplished directly by electrical resistance (for a conducting material) or indirectly by using an external heat source. Direct heating allows localized uniform heating by controlling either AC or DC current flow through the surface. While AC current is more energy efficient, DC current allows more precise control of the surface temperature because response times are longer, i.e., making fine adjustments is easier in practice when heating a metal surface with DC current. A nickel strip with dimensions of 10.2 cm  $\times$  2.54 cm  $\times$  0.013 cm requires  $\sim 600$  W to reach a temperature of 1500 K.

Indirect heating of a surface to 1500 K necessitates that the elements operate at much higher temperatures. Silicon carbide, molybdenum disilicide, and tantalum heaters can be used at temperatures up to 1900 K. However, it is difficult to fabricate silicon carbide and molybdenum disilicide heaters in small sizes (areas less than 4 cm<sup>2</sup>), and heater elements often droop and sag when hot. Tantalum heaters become brittle when exposed to atmospheric oxygen and thus require frequent replacement. These considerations, coupled with the requirement for uniform heating of the ignition surface, favor direct heating methods over indirect approaches.

### 2.4. Fuel Delivery Assembly

A fuel/air mixture can be directed onto the heated ignition surface via an open or closed delivery system with either a continuous or batch flow process. For the measurements described here an open, continuous flow arrangement was

---

adopted which utilizes a commercial burner for delivering the fuel/air mixture to the surface. In such a system the fuel/air flow is constantly renewed, and the temperature of the heated surface can be continuously and slowly increased until ignition occurs. Upon ignition, the observation of a flame, which is sustained by the continued fuel/air flow, clearly marks the ignition point. The size of the fuel/air flow system can be matched to that of the ignition surface. An open fuel/air delivery scheme also allows easy access for other diagnostic measurements. The only significant drawbacks of an open system are the inability to investigate autoignition phenomena as a function of pressure and the possibility of the ignition causing flame propagation back to the fuel supply. A flashback arrestor is straightforward to incorporate into a continuous flow arrangement.

Closed systems and batch processing were also considered. However, ignition in an enclosure would initiate an explosion, typically requiring replacement of a blowout panel after each measurement. In addition, such a design would largely prevent the use of diagnostic techniques involving gas chromatography, mass spectrometry, and lasers. Batch processing leads to significant fuel decomposition as the temperature is increased prior to ignition, resulting in the measurement of an ignition temperature for pyrolysis products mixed with remnants of the original fuel. Of course, if the temperature ramp-up times are short, less decomposition occurs. However, faster temperature increases compromise precise determinations of the autoignition temperature.

## 2.5. Temperature Measurement

Optical pyrometers, film thermocouples, and bead thermocouples all cover the temperature range of interest for autoignition temperature determinations,  $\sim 500$ – $1500$  K. However, thermocouple measurements must be designed to minimize disturbing the flow or influencing the ignition event, for example by mounting behind the heated surface. In this case the thermocouple does not measure the ignition temperature directly but monitors a temperature closely proportional to that of the surface. Sheathed, beaded thermocouples were used in the present investigation to monitor surface temperatures. Advantages include ease of replacement, fast response time for small bead sizes, and modest cost. Sheathing the thermocouple in a durable material, such as stainless steel, increases the useful lifetime without sacrificing performance. Routine temperature measurements with an optical pyrometer provide a means to check the thermocouple values.

Film thermocouples, which have been developed to monitor cylinder wall temperatures in internal combustion engines [Kreider, 1986, 1989; Yust and

Kreider, 1989], were also considered. These devices are designed to have the same coefficient of thermal expansion as the surface to be monitored in order to maintain contact with the hot surface as the local temperature changes. In the present investigation the development of different formulations for each of the three metal surfaces would have been expensive and time consuming. Even if the appropriate formulations were available, it is likely that bonding the film thermocouple to the ignition surface would alter the surface properties sufficiently to affect the measured ignition temperature.

An optical pyrometer focused on the heated surface does not intrude upon the ignition process, but changing surface conditions, such as oxide formation on hot metal surfaces, could influence the temperature measurements by altering the surface emissivity. Certain types of optical pyrometers, such as the disappearing filament design, are too slow and cumbersome for routine measurement of a changing surface temperature. A two-color pyrometer could be utilized for continuous data collection, so long as the emissivity of the ignition surface remained constant.

### 3. APPARATUS FOR MEASURING AUTOIGNITION TEMPERATURES

#### 3.1. Apparatus Components

Figure 1 presents the schematic layout of the autoignition apparatus, which includes direct current power supplies, a foil holder, fuel and air flow controllers, a premixed flame burner assembly, bubblers to vaporize liquid fuels, and a data acquisition computer. Important features of our apparatus include the following: *Short duration test* - The contact time for the fuel/air mixture on the heated surface is kept constant and is estimated to be less than 150 ms. *Surface Heating* - The ignition surface is heated to 1500 K in a uniform and controlled manner. The experimental approach allows multiple measurements to be made with excellent repeatability. *Ignition criterion* - The visual appearance of a burner-stabilized flame establishes a reproducible and reliable indication of ignition. *Premixed flame burner* - Premixing of the fuel and oxidizer (dry air) provides a straightforward means to vary the fuel/air stoichiometry easily, and appropriate burner design also prevents flashback after ignition has occurred. The flow of fuel and air can be shrouded in order to maintain the desired stoichiometry. *Open system* - An open system avoids possible explosion hazards upon ignition and also provides access for mass spectrometric sampling and optical measurements should these be desirable. For example, recent

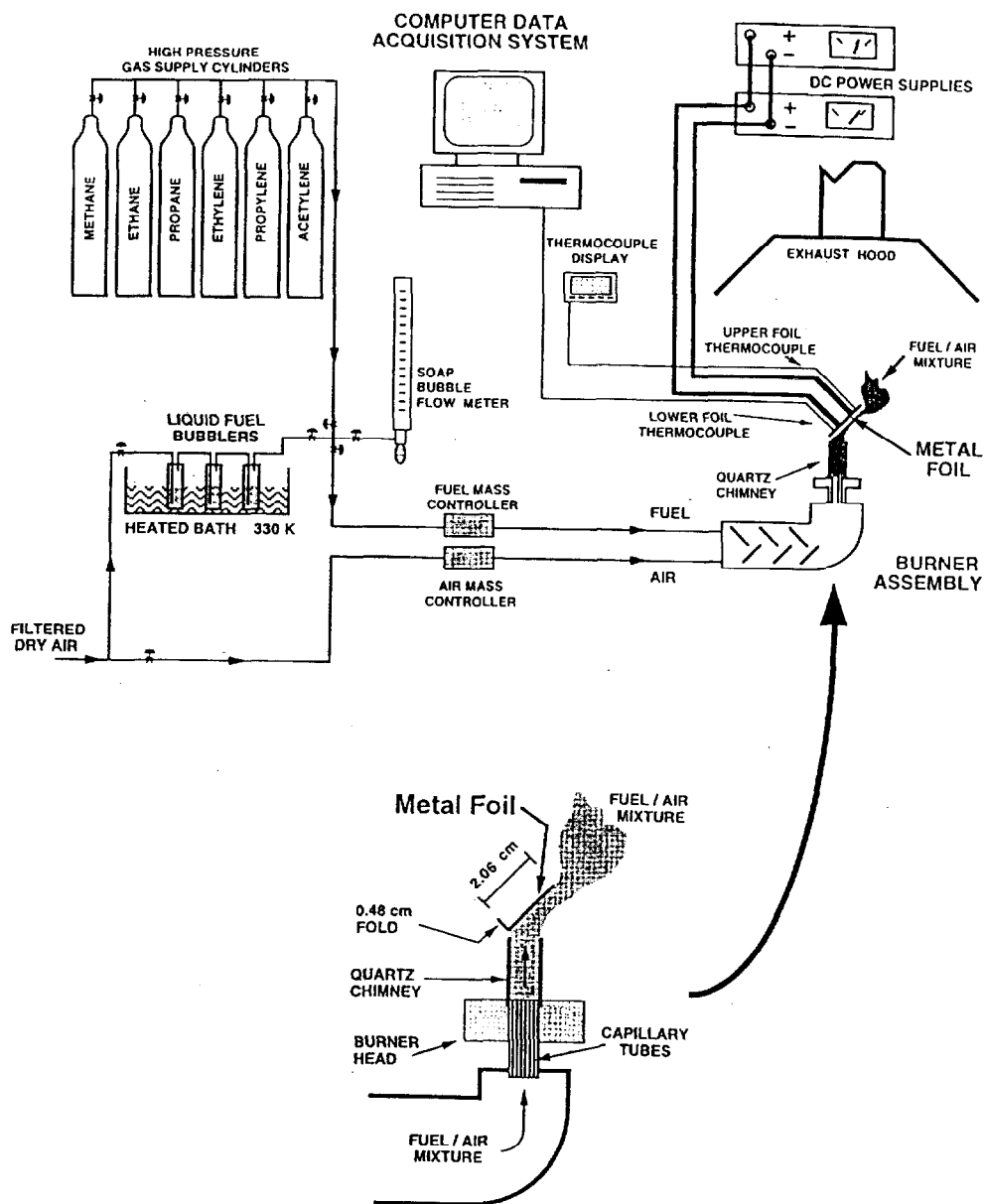


FIGURE 1 Schematic diagram of the apparatus for making short-duration autoignition temperature measurements using heated metal surfaces. Details of the preparation and mounting of the metal foils are described in Section 3.2.1.

autoignition investigations have included the detection of hydroxyl radical ( $\text{OH}\cdot$ ) [Pfefferle *et al.*, 1989a], O atom [Pfefferle *et al.*, 1989b], and formaldehyde [Bäuerle *et al.*, 1994]. There are two key elements in the present apparatus: the premixed flame burner and the holder for the thin metal foils.



### 3.1.1. Premixed Flame Burner

The burner assembly consists of a mixing chamber and a custom burner head of 1.1-cm diameter made from 61 capillary tubes to prevent flashback upon ignition. This configuration allows a known and easily variable mixture of hydrocarbon fuel and air to be directed toward the hot metal surface (see Fig. 1). Flow controllers are used on both the air and fuel streams. A 2.2-cm long by 1.1-cm diameter quartz chimney isolates the fuel/air mixture from ambient air; at the chimney exit the distance from the center of the flow to the hot surface is 0.64 cm. The lighter hydrocarbons are drawn from high-pressure gas cylinders and mixed with dry filtered air to achieve the desired stoichiometry. For the heavier hydrocarbons, which have lower vapor pressures, the liquid hydrocarbon is placed in glass bubblers located in a 330 K water bath,  $\sim 35$  degrees above ambient conditions. The temperature and pressure of the bubblers determine how much hydrocarbon vapor is introduced into the air stream. In our experiments the temperature is fixed for each liquid fuel, and part of the combustion air passes through a series of three bubblers to ensure saturation. This portion is then mixed with the appropriate amount of air within the burner assembly to obtain the desired stoichiometry. Once ignition occurs, the appearance of the burner-stabilized flame establishes a reproducible and reliable ignition criterion. The onset of ignition is detected both visually and by thermocouple readings.

Operating at low fuel flow rates is desirable. Fuel vapor pressures decrease with increasing molecular weight, making it more difficult to vaporize sufficient quantities of the liquid hydrocarbon fuels to sustain burning once ignition occurs. Since the flow rate of the fuel/air mixture affects the contact time at the heated surface, a series of temperature measurements was conducted at cold flow velocities of 8, 12, 16, 24 and 32 cm/s (Section 3.2 describes the experimental procedures). These velocities are average values calculated by dividing the flow rate of the fuel/air mixture by the cross-sectional area of the quartz chimney ( $0.95 \text{ cm}^2$ ). Figure 2 shows that the observed autoignition temperatures for ethylene/air mixtures igniting on a nickel surface are relatively independent of the approach velocity for our experimental set-up. Hamins and Borthwick [1997] have recently repeated these measurements and have also found that the autoignition temperatures are insensitive to the reactant flow velocity. In addition, they found that there was no effect of the angle between the mean flow of an ethylene/air mixture and the nickel foil until they reached  $90^\circ$ , where the measured autoignition temperature dropped by almost 100 K, presumably due to increased contact time at the stagnation point. These observations suggest that the rate-limiting chemical and transport

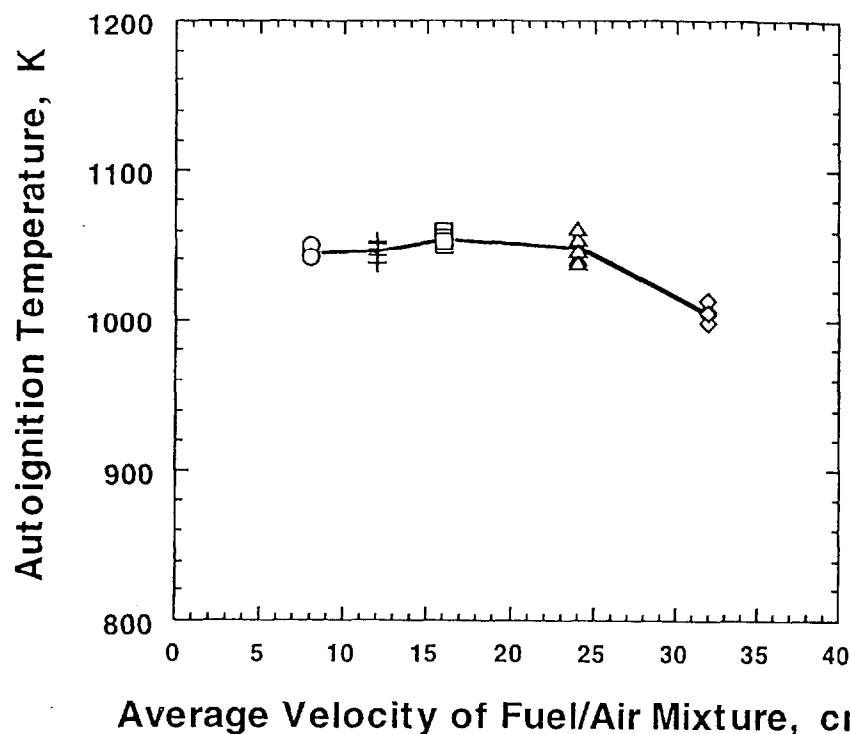


FIGURE 2 Measured autoignition temperatures as a function of the flow velocity for ethylene/air mixtures ( $\phi = 1.0$ ) on a heated nickel surface.

processes occur in the boundary layer which develops along the heated surface [Sano and Yamashita, 1994].

A fuel/air velocity of 16 cm/s was selected for making all of the autoignition temperature measurements reported here. With this flow velocity at the exit of the quartz chimney located above the burner, the total volumetric flow rate was 15.2 cm<sup>3</sup>/s and the fuel/air mixture flowed near the heated surface for an estimated 130 ms. This value of the contact time is simply obtained from the approach velocity (16 cm/s) and the exposed width of the heated surface (2.06 cm; see next section). Possible mixing effects are not included in the calculated contact time, nor is the influence of buoyancy induced by heating of the gas as it passes near the surface considered. As a result, the actual contact time is uncertain.

### 3.1.2. Holder for the Heated Metal Surface

Figure 3 shows the second key element of our apparatus, namely the holder for the thin metal foils, which also includes local temperature measurement capability. This holder was mounted on an adjustable arm in order to orient

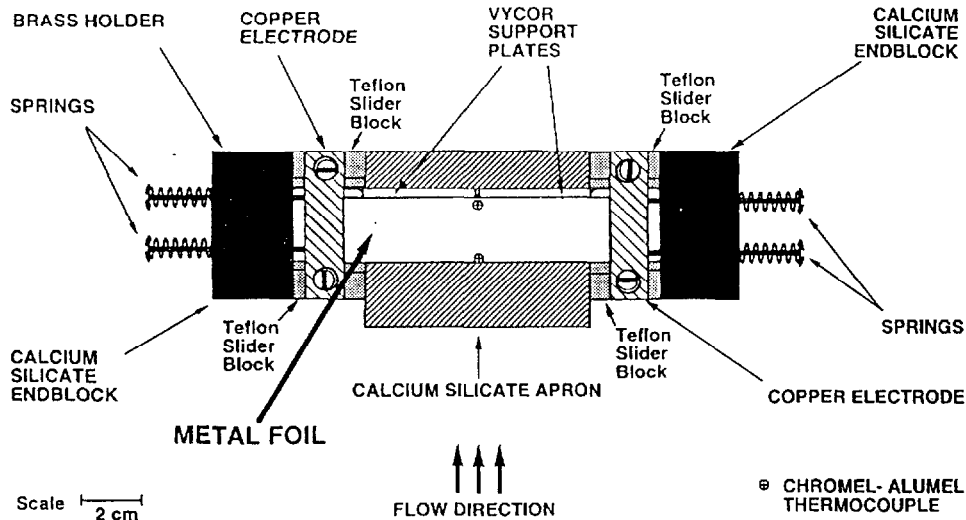


FIGURE 3 Schematic diagram of the holder for the thin metal foils.

the metal foil at an angle of  $45^\circ$  relative to the direction of the flow (Fig. 1). The temperature of the surface increases as the DC current passes through the foil (typical dimensions are  $10.2 \text{ cm} \times 2.54 \text{ cm} \times 0.013 \text{ cm}$ ). Approximately 40 amps at less than 20 V are necessary to heat the nickel foil to 1300 K. Although notching each foil at the lower edge on the centerline (see Section 3.2.1) forces the center portion to heat up more than the ends, the foil ends still become sufficiently hot that expansion can cause loss of electrical contact. This is prevented by spring loading the electrodes to maintain electrical contact as the foil expands. Since the foil also expands lengthwise, the holder utilizes a second set of springs to stretch the foil. This stretching preserves the  $45^\circ$  approach angle between the foil and the flow direction of the fuel/air mixture, helps to prevent gas flow behind the foil, and maintains good contact with the two Chromel-Alumel thermocouples positioned behind the foil. Note that the fuel/air mixture flows across the width of the metal foil (see Fig. 3).

The three materials selected for ignition surfaces were nickel (99.9%), stainless steel (304 series), and titanium (99.9%), purchased as  $2.54 \text{ cm} \times 10.2 \text{ cm}$  foil strips. These metals are widely used, and their cost and power requirements for heating are suitable for the present experiments. The electrical resistivities of the metals, which are 3, 9, and  $70 \mu\Omega\text{-cm}$  for nickel, stainless steel, and titanium, respectively [Marks, 1951], dictated foil thicknesses of 10, 12.7, and  $5.1 \mu\text{m}$  for the available DC power supplies. Attempts to use aluminum as an ignition surface failed because of its relatively low melting point. As the aluminum foil was heated to temperatures of  $\sim 800 \text{ K}$ , the foil began to melt and lose its tensile strength. The tension which was necessary to

hold the foil against the thermocouples separated the softened foil into two pieces.

### ***3.1.3. Temperature Measurement***

Fast response sub-miniature stainless steel sheathed Chromel-Alumel thermocouple probes (Omega, Stamford, CT\*) were used to monitor the foil temperatures, with an estimated response time of 0.4 s ( $1/e$  time [Omega, 1995]) and a recommended operating range of 75 K to 1530 K. Two thermocouples were placed in contact with the foil from behind, with the upper thermocouple positioned 0.16 cm below the upper edge of the foil and the lower thermocouple located 0.32 cm up from the lower edge (see Fig. 3). The thermocouple probes utilized 38  $\mu\text{m}$  wires within a 0.25-mm diameter 304 stainless steel sheath. Each thermocouple bead was electrically insulated from the sheath with magnesium oxide. These insulated or ungrounded thermocouples were necessary to isolate the temperature voltage (mV) from the heating voltage (up to 20 V). As the thermocouple probes were exposed to the hot surfaces, thermal and mechanical stress eventually caused the 38  $\mu\text{m}$  wires to become brittle, necessitating periodic replacement.

### ***3.1.4. Liquid Fuel Vaporization***

Liquid fuels were vaporized by saturating a portion of the air stream, which was bubbled through washing bottles filled with the fuel. The appropriate amount of fuel needed to obtain overall stoichiometries of 0.7, 1.0, and 1.3 was determined from published values of vapor pressure versus temperature [Jordan, 1954]. Four pairs of 125-mL glass bubblers were arranged in parallel in order to reduce the air flow rate and optimize equilibration of the fuel's vapor pressure at the local temperature in each bubbler. Breaking the gas flow up into many small bubbles via fritted glass sparging disks also helped to saturate the air stream with fuel by maximizing the bubble surface area. The air/fuel flow from the four pairs of bubblers was then collected into a single 500 mL bubbler, and thus each air stream passed through a total of three bubblers. A pressure tap on the 500 mL collection bubbler monitored the pressure above the liquid fuel. An insulated water bath was employed to keep the bubblers at a

---

\*Certain commercial equipment is identified herein in order to adequately specify the experimental procedure. Such identification does not imply recommendation by the National Institute of Standards and Technology, nor does it imply that this equipment is the best available for the purpose.

specific temperature, using a circulation pump to constantly mix the bath while three heaters maintained the desired water temperature, monitored using a submerged Chromel-Alumel thermocouple. In each of the four parallel lines, the first bubbler was operated at room temperature, typically  $298 \pm 3$  K, while the second was placed in the water bath, along with the large collection bubbler. Moderate increases in temperature, up to 330 K, were necessary to raise the vapor pressure of the heavier liquid fuels to obtain the needed flow rates. In order to minimize the condensation of fuel inside the fuel delivery lines between the bubblers and the burner head, the lines were kept as short as possible and warmed using resistance tape heaters.

Laboratory constraints necessitated long fuel supply lines in the 1994 series of measurements, leading to fuel condensation problems for the higher molecular weight fuels (larger than  $C_5$ ). For improved vaporization of these fuels, a heated brass tee/syringe pump system was used (instead of the bubbler arrangement), located close to the burner head. A small brass tee (0.623-cm diameter) was wrapped with resistance tape heaters and packed with fiberglass in order to maximize the surface area available for vaporization. A metered flow of pressurized air was introduced into one leg of the tee, while a syringe pump injected liquid fuel through a second branch at precise and very low fuel flow rates ( $< 2$  mL/minute). The resulting mixture of fuel and air exited through the third leg of the tee to the burner. The temperature of the brass tee was typically set 5 K above the boiling point of the fuel. A specific air flow rate was selected and the fuel delivery rate adjusted to reach the desired stoichiometry of the fuel/air mixture.

### **3.1.5. Data Acquisition System**

Data acquisition utilized a Metrabyte DASCON-1 multifunctional analog/digital expansion board, which featured four input/output channels with 12-bit resolution. For each temperature data point the computer recorded five thermocouple voltages, averaged the values, converted the voltage to a temperature, and reported a single value at approximately 0.5 s intervals. A cold junction compensator in the thermocouple line eliminated the need for a reference thermocouple. The computer also recorded a second channel which was used to mark each ignition event. When not activated, the marker channel voltage was less than 1 volt. Upon visual observation of ignition, a push-button was manually depressed and the marker channel voltage was increased to  $\sim 1.5$  V. The subsequent peak in the marker channel voltage identified each ignition event. At each time step the computer recorded the time, the thermocouple temperatures, the marker channel voltage, and the

step number. Figure 4 is an example of the data plotted for a single ignition event; the autoignition temperature is determined from the intersection of lines marking the ignition event and the time versus temperature record (also see Section 3.2.5).

## 3.2. Experiment Procedures

### 3.2.1. Foil Preparation

Before mounting on the holder, a small semi-circular notch (depth = 0.32 cm and radius of curvature = 1.27 cm) was removed from the center of the lower edge of each foil. This notch reduced the cross sectional area for current flow and forced heating to occur preferentially at the center of the foil, thus creating an area on the surface of localized uniform heating. Without this notch, foil imperfections or strain associated with stretching caused non-uniform and unpredictable hot zones. A 0.48-cm wide strip along the lower edge was folded over at 90°, and as the foil was mounted on the holder, 0.32 cm of this lip slipped into a recessed slot. This arrangement minimized flow disturbances,

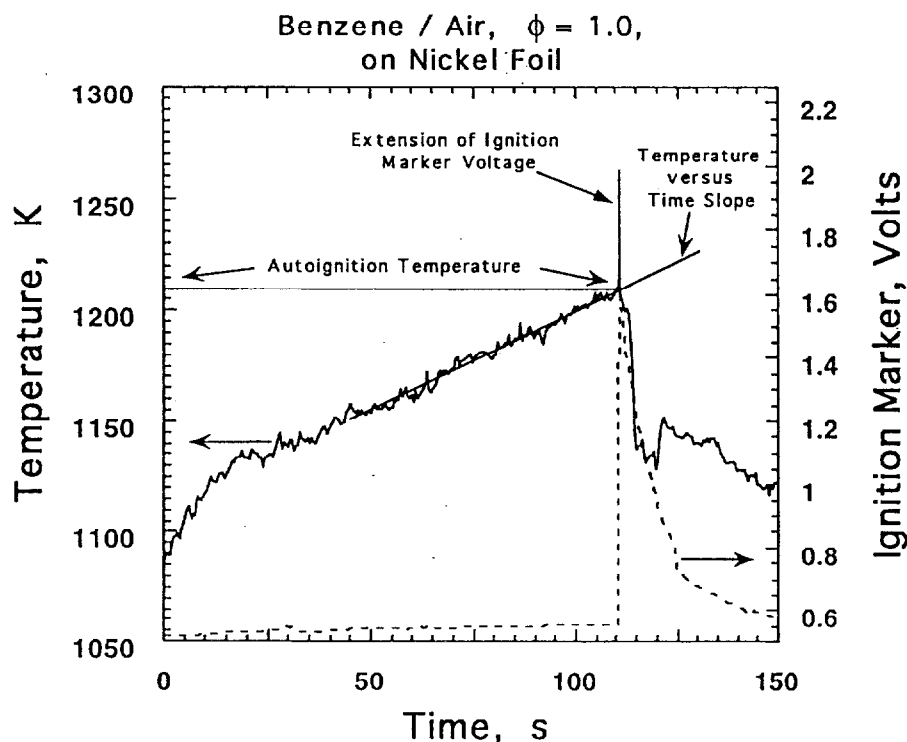


FIGURE 4 Determination of the autoignition temperature from the temperature vs. time record for a benzene/air mixture ( $\phi = 1.0$ ). Also shown is the voltage record of the ignition marker. The intersection of the two lines indicates the autoignition temperature.

reduced the flow of the fuel/air mixture behind the foil, and improved the foil stretching characteristics. The partially recessed leading edge of the foil thus included the notch, giving an exposed foil length along the flow direction of 2.06 cm (i.e., the foil width of 2.54 cm minus the 0.48 cm folded portion).

### ***3.2.2. Foil Mounting and Burn-in***

After each foil was notched, trimmed, and folded, it was placed on the holder and positioned over the two thermocouples. Before tightening the electrode springs, stainless steel shims were inserted with the foil ends to provide a better grip. After tightening the electrode springs, the stretching springs were adjusted to stretch the foil over the thermocouples. The DC current was then adjusted to heat the foil in 50–75 K steps. As the temperature of the foil increased, the foil expanded and began to move away from the supporting thermocouples. At this point the current was turned off, the foil was re-tightened, and the current was quickly turned on again before the foil cooled to ambient temperature.

As each foil was burned in, the current values and foil temperatures were recorded. Nickel and titanium usually did not require much tightening after the initial mounting. The stainless steel stretched and expanded to a much greater extent and required several iterations of heating up to  $\sim 900$  K, tightening, heating, and further tightening. Typically the lower thermocouple reported temperatures 50 to 100 K higher than the upper thermocouple, due to the increased current flow near the notch in the foil. The upper thermocouple was used only as a check that the apparatus was operating properly.

### ***3.2.3. Flow Measurement, Calibration, and Calculation***

Small rotameters and mass flow controllers were used to control the flow rate of the hydrocarbon fuels and the air for combustion. In addition, the back side of the foil mounting block (fabricated of calcium silicate) and the electrodes were cooled by air streams to reduce thermal stress on the components. Before each ignition series a soap bubble flowmeter was utilized to calibrate the smaller flow rate, usually the fuel flow. Periodically, a large soap bubble flowmeter was used to calibrate the air flow rate. For the heavier hydrocarbons almost all the combustion air was passed through the bubblers, so the mass controllers monitored both the fuel and air flow in these cases.

Each hydrocarbon fuel was ignited under stoichiometric fuel/air conditions ( $\phi = 1.0$ ), determined by assuming complete conversion of the fuel to carbon dioxide and water. Most of the fuels were also ignited under lean ( $\phi = 0.7$ ) and

rich conditions ( $\phi = 1.3$ ). Fuel flow rates were typically steady and did not drift significantly over the 10 to 15 minutes required for an ignition series, during which the flow rate was set but not adjusted. Fuel and air flows were established to provide a total flow rate of  $15.2 \text{ cm}^3/\text{s}$  through the burner, thus keeping the cold flow velocity at  $16 \text{ cm/s}$  for all fuels and stoichiometries (see Section 3.1.1).

Calibrating the fuel flow rates for the liquid hydrocarbons followed the same procedure as for the gaseous fuels, but included vapor pressure calculations. Prior to a series of ignition measurements an atmospheric pressure reading was obtained from a mercury barometer, and the vapor pressure of the hydrocarbon fuel was obtained from tabulations of vapor pressure versus temperature [Jordan, 1954]. Using the atmospheric pressure, the fuel vapor pressure at the temperature of the water bath, and the desired stoichiometry, the appropriate flow rate through the bubblers was calculated and the flow was adjusted to this value. With the flow rate near the final expected value, the bubbler pressure was recorded and included with the vapor and ambient pressures in a second fuel flow rate calculation.

The calculations outlined above are based on the assumption that the air passing through the bubblers was completely saturated. This was checked by monitoring the volumetric flow rates and the pressure on the final collection bubbler. The fraction of the liquid fuel in the bubbler flow was taken to be equal to the vapor pressure of the fuel divided by the sum of the atmospheric and bubbler pressures. Dividing the volumetric flow rate of pure fuel for a specified stoichiometry by this fraction of the fuel in the bubbler flow determined the flow rate of air which must be supplied to the bubblers to provide the required amount of fuel at the burner. Subtracting the bubbler flow rate from the total flow rate yielded the flow rate for the combustion air necessary for the specified stoichiometric conditions. The bubbler flow rates were calibrated before each ignition series using the soap bubble flowmeter.

#### ***3.2.4. Ethylene Benchmark Autoignition Temperature Measurements***

After each foil was mounted and burned in, an ignition series using an ethylene/air mixture was conducted to help characterize foil performance. This benchmark ethylene series also provided comparison of different samples of the same foil material. The ethylene ignitions allowed for final adjustments and checks of the foil, the sample holder, and the thermocouples before actually making autoignition temperature measurements for the specific hydrocarbon fuels.



### 3.2.5. Autoignition Temperature Measurements

After making the ethylene benchmark temperature measurements, each fuel/air mixture was introduced onto the heated metal surface. The surface temperature was increased at a rate of  $\sim 1$  K/s until ignition occurred. This first or zeroth ignition was monitored but not recorded for future data analysis. The zeroth ignition helped to define a temperature range where subsequent ignitions were probable and was used to establish a reasonable initial foil temperature 50 to 75 K below the ignition temperature. After adjusting the foil to this initial temperature, the data acquisition system was reset and a series of 5 ignitions was initiated. Typically the fuel/air mixture was allowed to flow and equilibrate for 45 s. After this equilibration time the surface temperature was increased by  $\sim 0.5$  K/s until ignition occurred. After ignition, the fuel flow and occasionally the air flow were shut down to extinguish the flame. This normally required less than 15 s. The fuel and air flow were then restarted and allowed to equilibrate for 45 s before again ramping up the surface temperature. Five repeat temperature measurements required from 8 to 19 minutes to complete, with a typical ignition series lasting about 12 minutes.

Surface temperatures were also checked with an optical pyrometer, which utilized the disappearing filament design (The Pyrometer Instrument Co., Bergenfield, NJ). When the disappearing filament was positioned close to the lower thermocouple, the pyrometer temperatures were found to be 50–60 K higher than the thermocouple values for typical operating conditions ( $T = 1000$ – $1300$  K). Some local cooling of the heated foil was evident by the appearance of dark spots at the positions of the thermocouples. All temperature values reported in the next section are the thermocouple determinations.

After each ignition series the temperature versus time data were plotted along with the marker channel versus time record. As illustrated in Figure 4, the autoignition temperature was determined for each plot from the intersection of a line drawn through the temperature versus time data which approximated the slope of the curve just before ignition and a vertical line indicating the ignition time identified by the marker channel.

## 4. RESULTS

Table I summarizes the 1990 autoignition temperature data for 15 hydrocarbon fuels on heated nickel, stainless steel, and titanium surfaces at three stoichiometries. The entries are averaged temperature values with a stated

TABLE I Measured Autoignition Temperatures (K)

| Fuel              | Nickel Foil   |               |               | Stainless Steel Foil |               |               | Titanium Foil |               |               |
|-------------------|---------------|---------------|---------------|----------------------|---------------|---------------|---------------|---------------|---------------|
|                   | $\phi = 0.7$  | 1.0           | 1.3           | 0.7                  | 1.0           | 1.3           | 0.7           | 1.0           | 1.3           |
| Methane           | 1367 $\pm$ 6  | 1313 $\pm$ 10 | 1247 $\pm$ 22 | 1252 $\pm$ 4         | 1087 $\pm$ 8  | 941           | 1332          | 1311 $\pm$ 8  | 1249 $\pm$ 10 |
| Ethane            | 1171 $\pm$ 6  | 1169 $\pm$ 18 | 1158 $\pm$ 33 | 1049 $\pm$ 5         | 1040 $\pm$ 3  | 1041 $\pm$ 7  | 1104 $\pm$ 14 | 1083 $\pm$ 34 | 1067 $\pm$ 14 |
| Ethylene          | 1133 $\pm$ 6  | 1076 $\pm$ 24 | 1125 $\pm$ 6  | 1035 $\pm$ 5         | 988 $\pm$ 20  | 1025 $\pm$ 10 | 1054 $\pm$ 10 | 1041 $\pm$ 24 | 1002 $\pm$ 8  |
| Acetylene         | 1031 $\pm$ 5  | 984 $\pm$ 5   |               | 945 $\pm$ 10         | 935 $\pm$ 3   |               | 944 $\pm$ 49  | 928 $\pm$ 4   |               |
| Propane           | 1187 $\pm$ 4  | 1255 $\pm$ 7  | 1166 $\pm$ 7  | 1076 $\pm$ 4         | 1078 $\pm$ 4  | 1078 $\pm$ 4  | 1196 $\pm$ 17 | 1120 $\pm$ 8  | 1063 $\pm$ 15 |
| Propylene         | 1278 $\pm$ 6  | 1277 $\pm$ 9  | 1288 $\pm$ 23 | 1103 $\pm$ 10        | 1086 $\pm$ 6  | 1030 $\pm$ 4  | 1193 $\pm$ 3  | 1182 $\pm$ 10 | 1202 $\pm$ 5  |
| Butane            | 1201 $\pm$ 4  | 1212 $\pm$ 5  | 1228 $\pm$ 2  | 1070 $\pm$ 6         | 1057 $\pm$ 5  | 1048 $\pm$ 5  | 1154 $\pm$ 9  | 1080 $\pm$ 6  | 1094 $\pm$ 5  |
| 1-3 Butadiene     | 1242 $\pm$ 2  | 1232 $\pm$ 6  | 1225 $\pm$ 11 | 1039 $\pm$ 5         | 1028 $\pm$ 4  | 1003 $\pm$ 7  | 1123 $\pm$ 10 | 1059 $\pm$ 10 | 1124 $\pm$ 18 |
| <i>n</i> -Pentane | 1207 $\pm$ 4  | 1214 $\pm$ 6  | 1212 $\pm$ 8  | 1051 $\pm$ 4         | 995 $\pm$ 7   | 1024 $\pm$ 6  | 1151 $\pm$ 10 | 1081 $\pm$ 4  | 1108 $\pm$ 9  |
| <i>n</i> -Hexane  | 1185 $\pm$ 6  | 1178 $\pm$ 5  | 1189 $\pm$ 5  | 1065 $\pm$ 3         | 1048 $\pm$ 6  | 1046 $\pm$ 4  | 1092 $\pm$ 15 | 1072 $\pm$ 8  | 1069 $\pm$ 10 |
| Benzene           | 1186 $\pm$ 3  | 1210 $\pm$ 4  | 1193 $\pm$ 6  | 1043 $\pm$ 11        | 1016 $\pm$ 6  | 1043 $\pm$ 12 | 1127 $\pm$ 19 | 1141 $\pm$ 1  | 1083 $\pm$ 7  |
| Cyclohexane       | 1270 $\pm$ 9  | 1204 $\pm$ 4  | 1195 $\pm$ 5  | 1084 $\pm$ 9         | 1061 $\pm$ 11 | 1071 $\pm$ 6  | 1133 $\pm$ 8  | 1108 $\pm$ 9  | 1114 $\pm$ 13 |
| <i>n</i> -Heptane | 1182 $\pm$ 9  | 1170 $\pm$ 6  | 1163 $\pm$ 7  | 1079 $\pm$ 10        | 1062 $\pm$ 9  | 1086 $\pm$ 6  | 1129 $\pm$ 12 | 1123 $\pm$ 11 | 1180 $\pm$ 9  |
| <i>n</i> -Octane  | 1193 $\pm$ 19 | 1166 $\pm$ 10 | 1099 $\pm$ 22 | 1103 $\pm$ 17        | 1099 $\pm$ 8  | 1055 $\pm$ 8  | 1164 $\pm$ 7  | 1150 $\pm$ 11 | 1156 $\pm$ 4  |
| iso-Octane        | 1414 $\pm$ 23 | 1226 $\pm$ 10 | 1250 $\pm$ 5  | 1123 $\pm$ 10        | 1112 $\pm$ 9  | 1114 $\pm$ 3  | 1219 $\pm$ 8  | 1163 $\pm$ 10 | 1173 $\pm$ 17 |

Notes:  $\phi$  is the fuel/air ratio, where  $\phi = 1.0$  represents stoichiometric conditions for complete combustion to yield CO<sub>2</sub> and H<sub>2</sub>O. Thermocouple values are reported; the actual surface temperatures are estimated to be 50–60 K higher (see Section 3.2.5). The quoted uncertainties represent one standard deviation for repeat measurements.

uncertainty of one standard deviation for typically at least five repeat measurements. All the ethylene benchmark runs are included in Table I at  $\phi = 1.0$ , where 90, 67 and 112 temperature determinations were made for nickel, stainless steel, and titanium, respectively. The repeatability of these measurements within a single ignition series on a given day is excellent, usually within a total range of 20 K and never exceeding a total variation of 48 K. For igniting a given hydrocarbon fuel on different pieces of the same foil material and using different thermocouples, the maximum month to month (foil to foil) variations were found to be 61–64 K for the nickel, stainless steel, and titanium surfaces.

Figure 5 illustrates our measurement repeatability for a series of five benzene ignitions on a nickel surface. The ignition temperature (see Section 3.2.5) is indicated for each curve; all five values lie within a narrow 10 K temperature range. Hamins and Borthwick [1997] used the same apparatus and also found that their autoignition temperature measurements were repeatable to within typically 10 K on a given day and lay within 40–50 K on different days. Their measured autoignition temperatures for stoichiometric methane, propane, and ethylene/air mixtures over a heated nickel surface were higher than the values reported in Table I by 70, 72 and 43 K, respectively. Given these results,

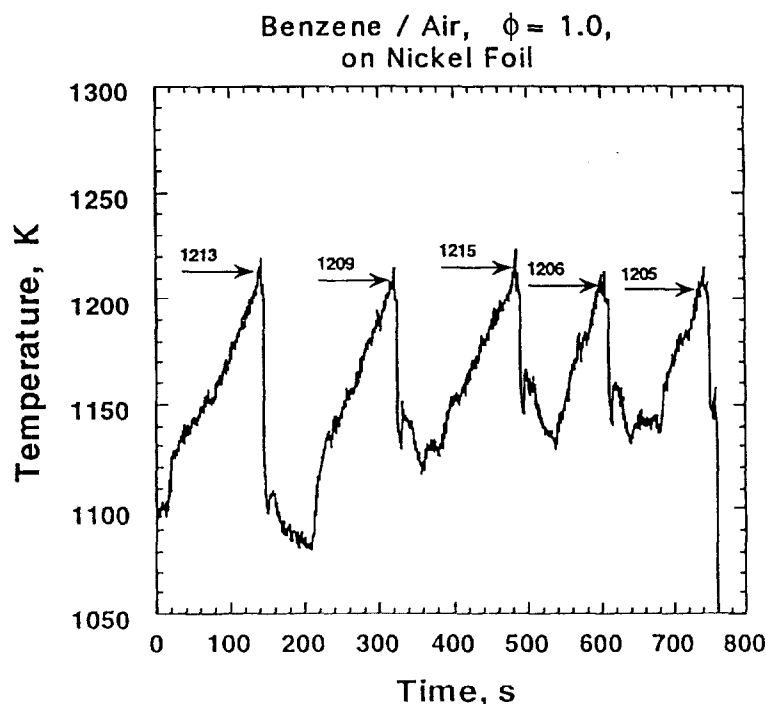


FIGURE 5 Temperature as a function of time for a benzene/air mixture ( $\phi = 1.0$ ) for five repeat determinations of the autoignition temperature using a heated nickel surface. The individual values of the autoignition temperature are shown.

small differences in autoignition temperatures ( $\sim 20$  K) between different fuels and surfaces can be reliably distinguished only in a series of measurements carried out with the same foil on the same day. Otherwise, only measured differences of 100 K or larger are meaningful.

Table II presents autoignition temperature results for the 1994 series of measurements, wherein five pairs of linear and branched alkanes are compared at stoichiometric conditions for a nickel surface. In general, the branched hydrocarbons exhibit higher autoignition temperatures, as expected (see below), but the observed differences are small. Also included are the results from the 1990 experiments, which are in close agreement with the later measurements.

Figure 6 presents data for ethylene and acetylene ignitions on a nickel surface over a more extended range of stoichiometries than investigated for the other fuels. These results show that the autoignition temperatures of both fuels decrease slowly for the richer fuel/air mixtures, a trend that was observed for most of the hydrocarbons investigated on the three metal surfaces (see Tab. I). In numerous fuel/surface/stoichiometry cases the autoignition temperatures exhibited a minimum at  $\phi = 1.0$ . In only one instance (propane on nickel) did the autoignition temperature exhibit a distinct maximum at  $\phi = 1.0$ .

Autoignition temperature measurements for acetylene are of interest because this fuel exhibits exceptionally wide flammability limits [Glassman, 1987], and the observed autoignition temperatures are the lowest of any fuel in

TABLE II Autoignition Temperatures for Linear and Branched Alkanes on Nickel Foil at  $\phi = 1.0$

| <i>Fuel</i>            | <i>Autoignition Temperature, K</i> |                    |
|------------------------|------------------------------------|--------------------|
|                        | <i>1990 Series</i>                 | <i>1994 Series</i> |
| Propane                | $1255 \pm 7$                       | $1233 \pm 9$       |
| Butane                 | $1212 \pm 5$                       | $1211 \pm 13$      |
| Isobutane              |                                    | $1226 \pm 15$      |
| <i>n</i> -Pentane      | $1214 \pm 6$                       | $1201 \pm 6$       |
| Methylbutane           |                                    | $1197 \pm 7$       |
| <i>n</i> -Hexane       | $1178 \pm 5$                       | $1221 \pm 5$       |
| 2,2-Dimethylbutane     |                                    | $1247 \pm 6$       |
| <i>n</i> -Heptane      | $1170 \pm 6$                       | $1188 \pm 10$      |
| 2,3-Dimethylpentane    |                                    | $1269 \pm 8$       |
| <i>n</i> -Octane       | $1166 \pm 10$                      | "                  |
| 2,2,4-Trimethylpentane | $1226 \pm 10$                      | $1235 \pm 7$       |

\*Measurements made only under lean conditions.

Notes: Thermocouple values are reported; the actual surface temperatures are estimated to be 50–60 K higher (see Section 3.2.5). The quoted uncer-

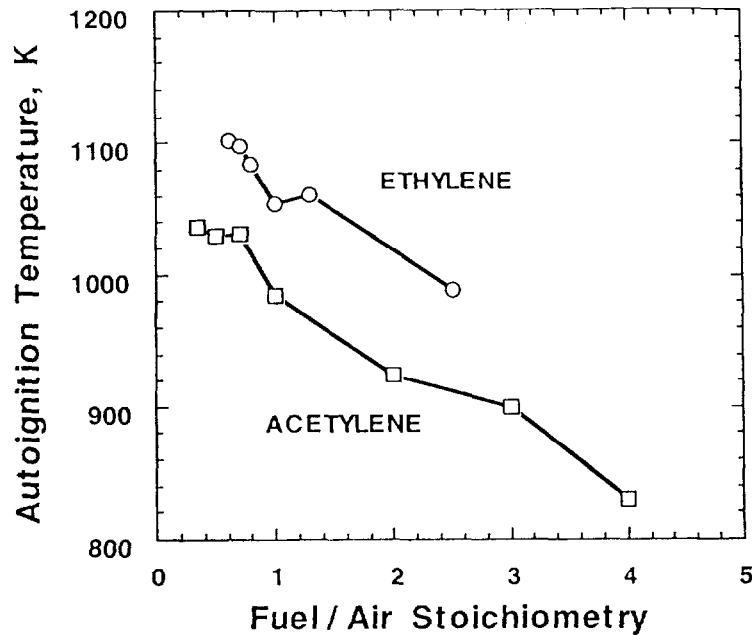


FIGURE 6 Measured autoignition temperatures on a nickel surface as a function of fuel/air stoichiometry for ethylene/air (open circles) and acetylene/air (open squares) mixtures.

this study. Additional measurements carried out for stainless steel and nickel surfaces [Smyth and Bryner, 1990] showed the same trend in the acetylene autoignition temperatures as illustrated in Figure 6 for  $\phi = 0.35$  to 4.0.

The variation of the measured autoignition temperatures with the heated metal surface is presented in Figure 7 for nickel, stainless steel, and titanium. All the data are shown for stoichiometric ( $\phi = 1.0$ ) ignition conditions. The highest temperatures are observed for the nickel surface, while the lowest are for stainless steel, often by as much as 200 K. The titanium data are intermediate. It is not clear how the different metal surfaces influence the measured autoignition temperatures.

## 5. DISCUSSION

### 5.1. Comparison with Literature Values

Autoignition temperatures have been measured previously for numerous pure hydrocarbons, with most of the recent published data acquired using the standard ASTM E659 procedure [1978]. Extensive compilations include those of Zabetakis *et al.* [1954], Mullins [1955], Zabetakis [1965], McCracken [1970], and the National Fire Protection Association [NFPA, 1995]. As mentioned earlier, this procedure often involves times extending up

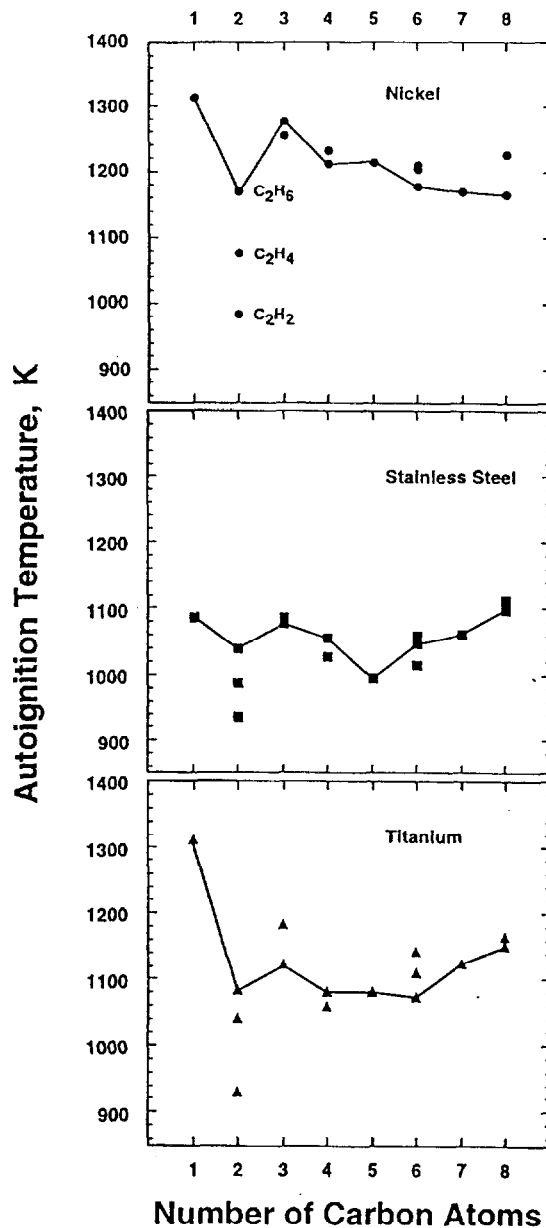


FIGURE 7 Measured autoignition temperatures as a function of carbon number for all of the fuels investigated ( $\phi = 1.0$ ). The data are shown for nickel (top), stainless steel (middle), and titanium (bottom) surfaces, with the low values labelled for the C<sub>2</sub> hydrocarbons (ethane, ethylene and acetylene; see also Tab. I). Straight lines connect the temperatures measured for the linear alkanes.

to several minutes [Setchkin, 1954; Zabetakis *et al.*, 1954], in contrast to the present measurements, where the contact time of the hydrocarbon vapor and the heated metal surface is estimated to be  $\sim 130$  ms.

Figure 8 compares literature data on autoignition temperatures from the compilation of the SFPE Handbook [NFPA, 1995, essentially the same data

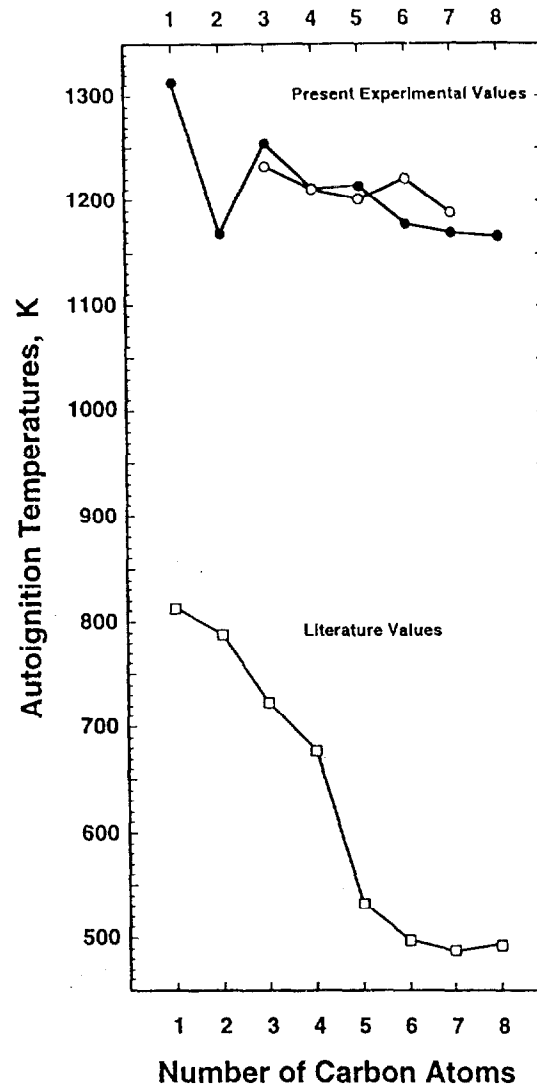


FIGURE 8 Comparison of measured autoignition temperatures as a function of carbon number for linear alkanes. Present experimental results: solid circles = 1990 measurements, open circles = 1994 measurements; all are for  $\phi = 1.0$ . Literature values (open squares) are from the SFPE Handbook of Fire Protection Engineering [NFPA, 1995], which are essentially the same as the values reported by Zabetakis [1965].

as that reported by Zabetakis (1965)] with our observed values on a nickel surface for the straight-chain alkane series. Our autoignition temperature measurements lie in the range of 928–1414 K for the 1990 series of 15 hydrocarbon fuels ignited by nickel, stainless steel, and titanium surfaces (Tab. I). As pointed out in Section 3.2.5, the actual surface temperatures are estimated to be  $\sim 50$ – $60$  K higher than the reported thermocouple values. Earlier results summarized by Mullins [1955], Zabetakis [1965], and McCracken [1970], as well as those shown in Figure 8, span a decidedly lower

range (481–910 K for glass surfaces), with no overlap in the data sets. Our temperature values are systematically higher by 500 K or more. The borosilicate surface employed in the ASTM procedure does not account for this difference. Pfefferle *et al.* [1989a, 1989b] report autoignition temperatures on quartz which are only  $\sim 110$ – $145$  K lower than they measured on platinum for lean ethane/air mixtures ( $\sim 1315$ – $1390$  K vs.  $\sim 1460$ – $1500$  K), and Coward and Guest [1927] found that platinum exhibited autoignition temperatures 100–150 K higher than any other metal surface for a range of stoichiometric conditions. These results suggest that the autoignition temperatures observed for a given fuel should be roughly similar for glass and non-catalytic metal surfaces. Therefore, the low autoignition temperatures reported in previous studies must arise from the long-contact time conditions inherent to the ASTM procedure, which promote fuel decomposition to yield products (such as acetylene) more easily ignited than the parent fuel.

Several investigators have also found high autoignition temperatures for experimental conditions which involve short contact times between the fuel/air mixture and the heated surface. Laurendeau and Caron [1982] measured autoignition temperatures for a lean methane/air mixture ( $\phi = 0.72$ ) under pulsed heating conditions, where the contact time was  $\leq 100$  ms. For a 10-mm wide stainless steel foil strip they report an ignition temperature of 1283–1293 K, which is close to our value of  $\sim 1300$  K (1252 K from Tab. I plus 50 K; see Section 3.2.5). Pfefferle *et al.* [1989a, 1989b] also measured high autoignition temperatures under short-contact time conditions, reporting values of  $\sim 1315$ – $1500$  K for lean ethane/air mixtures impinging upon quartz and platinum surfaces. Cutler [1974] measured very high autoignition temperatures ( $\geq 2000$  K) for methane in contact with a tungsten foil, where heating times were  $\leq 0.1$  ms.

## 5.2. Fuel Structure Effects

Experimental measurements of the autoignition behavior of hydrocarbon fuels all exhibit a critical dependence upon fuel structure [Zabetakis *et al.*, 1954; Mullins, 1955; Zabetakis, 1965; McCracken, 1970; NFPA 325M, 1984; NFPA, 1995]. Figure 8 reveals an overall trend toward lower autoignition temperatures with increasing chain length for both these prior measurements and for our results (with the exception of ethane,  $C_2H_6$ ; see below). For the linear hydrocarbons (methane to octane) the observed range of autoignition temperature values is compressed in our measurements relative to the results selected by the National Fire Protection Association [NFPA, 1995; essentially the same as Zabetakis (1965)]. However, the autoignition temperature values



compiled by Mullins [1955] and Zabetakis [1965] reveal a wide variation, often exceeding 250 K, for many hydrocarbon fuels. Setchkin [1954] and Zabetakis [1965] point out that the shape and size of the flasks used in these earlier experiments influence the measured autoignition temperature. Thus, it is difficult to make a more direct comparison of these data with the present measurements. Our results on stainless steel and titanium surfaces (Fig. 7) suggest that autoignition temperatures may increase for hydrocarbons larger than  $C_8$  molecules. A small increase in the autoignition temperatures of large alkanes (up to  $C_{20}$ ) has been reported by Frank and Blackham [1952] and by Zabetakis [1965] for their long contact time conditions.

Table I and Figure 8 show that the  $C_2$  hydrocarbons (ethane, ethylene, and acetylene) are anomalously easy to ignite in the present series of measurements, particularly acetylene. Zabetakis [1965] also reports a very low value for acetylene ( $\sim 578$  K). Detailed modeling studies which compare the autoignition behavior for a range of simple hydrocarbons are scarce. However, Mulholland *et al.* [1992] have analyzed the autoignition of several fuels using global ignition kinetics. For plug flow reaction conditions and a one second residence time, they predict autoignition temperatures of 990 K, 980 K, 950 K, and 750 K for methane, ethane, ethylene and acetylene, respectively. These values lie in the same order as our experimental results, and they are distinctly lower by an average of 218 K (as expected from the longer residence time). Zabetakis [1965] also found the same order in his earlier autoignition temperature measurements. The low autoignition temperature calculated for acetylene is attributed to the facile attack of this fuel by  $O_2$  to give two OH radicals [Mulholland *et al.*, 1992]. In accord with this prediction, Griffin *et al.* [1992] measured  $\cdot OH$  levels near a heated platinum surface significantly higher for acetylene than for methane and ethane. Lutz *et al.* [1988] used a detailed mechanism to calculate induction times for autoignition, finding an order of acetylene < ethane  $\sim$  ethylene < methane, in general agreement with our results.

Both experimental and modeling studies indicate that branched alkanes are more difficult to ignite than their linear isomers [Zabetakis *et al.*, 1954; McCracken, 1970; Pitz *et al.*, 1984; Dryer and Brezinsky, 1986; NFPA, 1995; Wilk *et al.*, 1990]. These observations are of special interest in terms of formulating safer fuels and in understanding the onset of engine knock [Minetti *et al.*, 1996]. Our 1994 measurements comparing branched and linear alkane ignition on a heated nickel surface are summarized in Table II. For short contact time conditions the branched alkanes do exhibit autoignition temperatures equal to or higher than their linear counterparts, but the observed differences are small. The largest increase for a branched vs. linear

fuel is only 80 K for the  $C_7$  hydrocarbons. Table I reveals that iso-octane exhibits higher autoignition temperatures for all three metal surfaces, with nickel showing the greatest contrast. Measurements made using the ASTM E659 and other similar methods (i.e., involving long contact times) again show larger differences [Zabetakis *et al.*, 1954; McCracken, 1970; NFPA, 1995].

As discussed above, our measurements exhibit a small decrease in the measured autoignition temperature of most hydrocarbons for rich conditions (see Tab. I and Fig. 6). Since the ASTM E659 test method does not control stoichiometry, comparison with most literature values cannot be made. Coward and Guest [1927] reported increasing autoignition temperatures under richer conditions for a wide variety of metal surfaces, in disagreement with the present results. Smith *et al.* [1984] predict that the autoignition temperatures of propane and *n*-butane should decrease slightly for richer conditions, due to the role of low temperature chemical reactions (additional fuel reacts to produce more  $H_2O_2$  and thus increase chain branching). Since hydrocarbon fuels inhibit their own oxidation (for example, see Westbrook *et al.* [1988]), autoignition will not occur until the fuel has been consumed. These considerations indicate that pre-ignition chemical effects influence autoignition behavior as a function of the fuel/air stoichiometry [Pitz and Westbrook, 1986; Morley, 1988; Westbrook *et al.*, 1988].

## 6. CONCLUSIONS

This study presents a new method for determining autoignition temperatures under steady flow conditions where the contact time between the fuel/air mixture and a heated metal surface is short ( $\sim 130$  ms) and the stoichiometry of the fuel/air mixture is well controlled. These measurements better establish the influences of fuel structure, mixture stoichiometry, and surface material than earlier experiments using the current ASTM procedure [1978], whose principal flaw is the lack of control over contact time. The present results are particularly relevant for applications involving brief contact times, such as accidents and malfunctions. However, measurements of autoignition temperatures for longer contact times are also of interest for evaluating hazards which involve extended durations. For example, long time experiments would be valuable in making conservative hazard assessments for long-term storage conditions. However, control of the contact time and mixture stoichiometry is required before one can make useful comparisons between different fuels and surface materials.

The autoignition temperatures reported here are found to be highly reproducible for a total of 19 hydrocarbon fuels ( $C_1$ – $C_8$ ) on nickel, stainless steel,

and titanium surfaces. As expected from prior studies, much higher autoignition temperatures are observed than in earlier investigations involving longer contact times. Our temperature values generally decrease for the larger hydrocarbons and for richer mixtures, with ethane, ethylene, and acetylene exhibiting anomalously low values, especially acetylene. Branched alkanes are more difficult to ignite than their linear isomers; as found in previous studies. The highest autoignition temperatures are observed for nickel surfaces and the lowest for stainless steel, with intermediate values obtained for titanium.

In terms of the range of autoignition temperatures for (1) different linear alkanes and (2) in comparing linear vs. branched alkanes, the present measurements exhibit a more narrow range than those made under long contact time conditions. This observation suggests that greater differences in the hydrocarbon pyrolysis decomposition products arise under relatively low-temperature, long duration conditions than for the present high-temperature, short contact time experiments.

### **Acknowledgements**

This investigation was originally supported by the Air Force Engineering and Services Center, Engineering and Services Laboratory, Tyndall Air Force Base, FL, under Contract Number JON 2104-3039 with Capt. John R. Floden as the project officer. The 1994 series of measurements was carried out at Tyndall using a second autoignition apparatus, with the assistance of Douglas Nelson (project officer) and Barry Mitchell. We thank William Bannister (University of Massachusetts at Lowell), who was instrumental in initiating this project with the Air Force, Thomas Norton (DOE Morgantown) for numerous insightful comments, Anthony Hamins (NIST) for stimulating discussions on autoignition temperature measurements, and Erik Johnsson (NIST) for his skillful participation in the second measurement series.

### **References**

- ASTM E659 (1978) Standard Test Method for Autoignition Temperature of Liquid Chemicals. This procedure replaced the older ASTM D2155 test.
- Bäuerle, B., Hoffman, F., Behrendt, F. and Warnatz, J. (1994) Detection of Hot Spots in the End Gas of an Internal Engine Using Two-Dimensional LIF of Formaldehyde. *Twenty-Fifth Symposium (International) on Combustion*, The Combustion Institute, Pittsburgh, PA p. 135.
- Coward, H. F. and Guest, P. G. (1927) Ignition of Natural Gas-Air Mixtures by Heated Metal Bars. *Journal of the American Chemical Society*, **49**, 2479.
- Cutler, D. P. (1974) The Ignition of Gases by Rapidly Heated Surfaces. *Combustion and Flame*, **22**, 105.

- Dryer, F. L. and Brezinsky, K. (1986) A Flow Reactor Study of the Oxidation of *n*-Octane and Iso-Octane. *Combustion Science and Technology*, **45**, 199.
- Frank, C. E. and Blackham, A. U. (1952) Spontaneous Ignition of Organic Compounds. *Industrial and Engineering Chemistry*, **44**, 862.
- Glassman, I. (1987) *Combustion*, Second Edition, Academic Press, San Diego; Appendix F: Spontaneous Ignition Temperature Data.
- Griffin, T. A., Calabrese, M., Pfefferle, L. D., Sappey, A., Copeland, R. and Crosley, D. R. (1992) The Influence of Catalytic Activity on the Ignition of Boundary Layer Flows. Part III: Hydroxyl Radical Measurements in Low-Pressure Boundary Layer Flows. *Combustion and Flame*, **90**, 11.
- Hamins, A. and Borthwick, P. (1997) Suppression of Ignition Over a Heated Metal Surface. *Combustion and Flame*, in press. Repeatability estimates from A. Hamins, personal communication (September, 1995).
- Holman, J. P. (1981) *Heat Transfer*, McGraw-Hill, New York, p. 169.
- Jordan, T. E. (1954) *Vapor Pressure of Organic Compounds*, Interscience Publishers, New York, Plates 1–10.
- Kreider, K. G. (1986) Thin Film Thermocouples for Internal Combustion Engines. *J. Vac. Sci. Technol. A*, **4**, 2618.
- Kreider, K. G. (1989) Thin Film Thermocouples for High Temperature Measurement. NISTIR 89-4087, U. S. Department of Commerce, National Institute of Standards and Technology, Gaithersburg, MD.
- Kumagai, S. and Kimura, I. (1957) Ignition of Flowing Gases by Heated Wires. *Sixth Symposium (International) on Combustion*. The Combustion Institute, Reinhold, New York, p. 554.
- Laurendeau, N. M. (1982) Thermal Ignition of Methane-Air Mixtures by Hot Surfaces: A Critical Examination. *Combustion and Flame*, **46**, 29.
- Laurendeau, N. M. and Caron, R. N. (1982) Influence of Hot Surface Size on Methane-Air Ignition Temperature. *Combustion and Flame*, **46**, 213.
- Lutz, A. E., Kee, R. J., Miller, J. A., Dwyer, H. A. and Oppenheim, A. K. (1988) Dynamic Effects of Autoignition Centers for Hydrogen and  $C_{1,2}$ -Hydrocarbon Fuels. *Twenty-Second Symposium (International) on Combustion*, The Combustion Institute, Pittsburgh, PA, p. 1683.
- Marks, L. S., editor (1951) *Mechanical Engineers' Handbook*, 5th edition, McGraw-Hill, New York, p. 1930.
- McCracken, D. J. (1970) Hydrocarbon Combustion and Physical Properties. BRL Report No.1496, Ballistic Research Laboratories, Aberdeen Proving Ground, MD.
- Minetti, R., Ribaucour, M., Carlier, M. and Sochet, L. R. (1996) Autoignition Delays in a Series of Linear and Branched Chain Alkanes in the Intermediate Range of Temperature. *Combustion Science and Technology*, **113–114**, 179.
- Morley, C. (1988) Photolytic Perturbation Method to Investigate the Kinetics of Hydrocarbon Oxidation Near 800 K. *Twenty-Second Symposium (International) on Combustion*, The Combustion Institute, Pittsburgh, PA, p. 911.
- Mulholland, J. A., Sarofim, A. F. and Beér, J. M. (1992) On the Derivation of Global Ignition Kinetics from a Detailed Mechanism for Simple Hydrocarbon Oxidation. *Combustion Science and Technology*, **87**, 139.
- Mullins, B. P. (1955) Spontaneous Ignition of Liquid Fuels. AGARDograph No.4, Butterworths, London, Chapter 11.
- NFPA 325M (1984) "Fire Hazard Properties of Flammable Liquids, Gases and Volatile Solids", National Fire Protection Association, Quincy, MA.
- NFPA (1995) National Fire Protection Association, *SFPE Handbook of Fire Protection Engineering*, Second Edition, Quincy, MA, p. 2–151.
- Omega (1995) *Omega Complete Temperature Measurement Handbook and Encyclopedia*, Stamford, CT, **29**, pp. A8 and Z43–44.
- Pfefferle, L. D., Griffin, T. A., Winter, M., Crosley, D. R. and Dyer, M. J. (1989a) The Influence of Catalytic Activity on the Ignition of Boundary Layer Flows. Part I: Hydroxyl Radical Measurements. *Combustion and Flame*, **76**, 325.
- Pfefferle, L. D., Griffin, T. A., Dyer, M. J. and Crosley, D. R. (1989b) The Influence of Catalytic Activity on the Ignition of Boundary Layer Flows. Part II: Oxygen Atom Measurements. *Combustion and Flame*, **76**, 339.

- Pitz, W. J., Westbrook, C. K., Proscia, W. M. and Dryer, F. L. (1984) A Comprehensive Chemical Kinetic Reaction Mechanism for the Oxidation of *n*-Butane. *Twentieth Symposium (International) on Combustion*. The Combustion Institute, Pittsburgh, PA, p. 831.
- Pitz, W. J. and Westbrook, C. K. (1986) Chemical Kinetics of the High Pressure Oxidation of *n*-Butane and its Relation to Engine Knock. *Combustion and Flame*, **63**, 113.
- Sano, T. and Yamashita, A. (1994) Flame Ignition of Premixed Methane Air Mixtures on a High-Temperature Plate. *JSME Intl. J., Series B*, **37**, 180.
- Setchkin, N. P. (1954) Self-Ignition Temperatures of Combustible Liquids. *Journal of Research of the National Bureau of Standards*, **53**, 49.
- Smith J. R., Green, R. M., Westbrook, C. K. and Pitz, W. J. (1984) An Experimental and Modeling Study of Engine Knock. *Twentieth Symposium (International) on Combustion*. The Combustion Institute, Pittsburgh, PA, p. 91.
- Smyth, K. C. and Bryner, N. P. (1990) Short-Duration Autoignition Temperature Measurements for Hydrocarbon Fuels. NISTIR 4469, U. S. Department of Commerce, National Institute of Standards and Technology, Gaithersburg, MD.
- Westbrook, C. K., Warnatz, J. and Pitz, W. J. (1988) A Detailed Chemical Kinetic Reaction Mechanism for the Oxidation of Iso-Octane and *n*-Heptane Over an Extended Temperature Range and Its Application to Analysis of Engine Knock. *Twenty-Second Symposium (International) on Combustion*, The Combustion Institute, Pittsburgh, PA, p. 893.
- Wilk, R. D., Pitz, W. J., Westbrook, C. K., Addagarla, S., Miller, D. L., Cernansky, N. P. and Green, R. M. (1990) Combustion of *n*-Butane and Isobutane in an Internal Combustion Engine: A Comparison of Experimental and Modeling Results. *Twenty-Third Symposium (International) on Combustion*. The Combustion Institute, Pittsburgh, PA, p. 1047.
- Yust, M. and Kreider, K. G. (1989) Transparent Thin Film Thermocouple. *Thin Solid Films*, **176**, 73.
- Zabetakis, M. G. (1965) Flammability Characteristics of Combustible Gases and Vapors. U. S. Bureau of Mines Bulletin 627.
- Zabetakis, M. G., Furno, A. L. and Jones, G. W. (1954) Minimum Spontaneous Ignition Temperatures of Combustibles in Air. *Industrial and Engineering Chemistry*, **46**, 2173.